# Structural Insight into Pre-B Cell Receptor Function

Alexander J. Bankovich, *et al.*

*Science* **316**, 291 (2007);
DOI: 10.1126/science.1139412



*Science* (print ISSN 0036-8075; online ISSN 1095-9203) is published weekly, except the last week in December, by the American Association for the Advancement of Science, 1200 New York Avenue NW, Washington, DC 20005. 

# Structural Insight into Pre-B Cell Receptor Function

Alexander J. Bankovich,[1] Stefan Raunser,[6] Z. Sean Juo,[2,3,4] Thomas Walz,[6] Mark M. Davis,[1,2,5] K. Christopher Garcia[1,2,3,4]*

The pre-B cell receptor (pre-BCR) serves as a checkpoint in B cell development. In the 2.7 angstrom structure of a human pre-BCR Fab-like fragment, consisting of an antibody heavy chain (HC) paired with the surrogate light chain, the "unique regions" of VpreB and λ5 replace the complementarity-determining region 3 (CDR3) loop of an antibody light chain and appear to "probe" the HC CDR3, potentially influencing the selection of the antibody repertoire. Biochemical analysis indicates that the pre-BCR is impaired in its ability to recognize antigen, which, together with electron microscopic visualization of a pre-BCR dimer, suggests ligand-independent oligomerization as the likely signaling mechanism.

B cells traverse regulatory checkpoints to ensure that their surface-expressed antigen-specific B cell receptor (BCR) is functional yet not autoreactive (*1*). Upon antigen recognition by the BCR, a B cell becomes activated, expands clonally, and advances to the plasma cell stage, where it secretes soluble antibody. Before antibody genes can be transcribed, each B cell must productively rearrange one HC and one light chain (LC) gene (*2*). After HC expression but before the LC is rearranged to form the mature BCR, the pre-BCR is expressed (*3*, *4*). In a functional pre-BCR, two invariant proteins, λ5 and VpreB, form a heterodimer called the surrogate light chain (SLC) that pairs with a rearranged HC (*5*–*10*).

Not all rearranged HCs can pair with the SLC to form a pre-BCR (*11*), but the structural basis of selection and pairing is unknown. In mice, only half of the in-frame rearranged HCs pair correctly with SLCs (*11*). Only those B cells that express an HC capable of pairing with the SLC undergo clonal expansion (*12*–*15*), which enriches for HCs that are capable of BCR formation (*16*). Humans that lack λ5 have a major block in B cell development, decreasing peripheral B cell numbers by more than 99% (*17*). λ5-deficient mice have a less severe phenotype, but B cell development remains substantially delayed (*18*).

The overall architecture of the pre-BCR is shown in Fig. 1A. The SLC/HC pair presumably contains a similar architecture of immunoglobulin (Ig)–like domains as a Fab, but the nonpolymorphic VpreB and λ5 are predicted to have divergent β-strand topologies in comparison to canonical Ig-domain sequences (*6*). The N terminus of λ5 and the C terminus of VpreB have "unique regions" that share no sequence similarity to known proteins nor have a counterpart in other Ig receptors. Yet, functional studies implicate these unique regions as being essential to pre-BCR function (*19*–*21*). Both the pre-BCR and BCR signal through interaction with a heterodimeric signaling complex, Igα/Igβ, which has intracellular segments containing immunoreceptor tyrosine-based activation motifs (ITAMs) that interact with downstream adaptor and effector molecules (*22*). In the mature BCR, antigen engagement leads to receptor clustering and activation. However, it remains unclear whether pre-BCR signaling during normal B cell development is ligand dependent. On the one hand, several putative extracellular ligands have been identified, such as galectin-1 in humans (*20*) and heparin sulfate in mice (*19*). On the other hand, unique region–dependent, homotypic pre-BCR aggregation alone is capable of initiating downstream signaling events (*21*).

To gain structural insights into pre-BCR biology, we expressed and crystallized a soluble form of the human pre-BCR analogous to the Fab of an antibody (dashed box in Fig. 1A). This "Fab-like" pre-BCR was secreted from baculovirus-infected insect cells by triple coinfection of recombinant viruses encoding an ovalbumin (OVA)–specific human HC [variable region of Ig HC ($V_H$) and domain 1 of the constant portion of the Ig HC ($C_H1$)], λ5, and VpreB. We crystallized a monomeric form of the pre-BCR with the λ5 N terminus truncated by 36 residues and determined the structure to 2.7 Å (the complex with intact λ5 forms a dimer that will be discussed later). The pre-BCR adopts an overall quaternary structure that is reminiscent of a Fab. The SLC heterodimer proteins VpreB and λ5 replace the Ig LC variable and constant regions ($V_L$ and $C_L$) of a Fab, respectively (Fig. 1B). The VpreB domain forms a canonical V-type Ig fold that includes β strands a to f (*23*). However, the VpreB polypeptide g strand is replaced by a portion of the N-terminal unique region of λ5 that completes the bottom β sheet of the V-type Ig fold (Fig. 1C). In this arrangement, the λ5 unique region substitutes for the J region of a normal $V_L$ that follows LC CDR3 (CDR3-L) and is involved in the $V_H/V_L$ interface. This strand swap, which was previously predicted from homology modeling (*5*, *24*), has no counterpart in Ig domains characterized to date. In accord with the obligate nature of SLC heterodimer formation (*7*), the interface between VpreB and the λ5 β strand is extensive, burying ~1000 Å$^2$ of surface area and forming 16 hydrogen bonds (Fig. 1D). The λ5 β strand exits from the base of VpreB and enters the λ5 constant domain. The λ5 structure is similar to a Fab $C_L$ domain (82% identity and 1.4 Å root mean square deviation).

The region of the pre-BCR that is analogous to the antigen-binding site of antibodies contains surface-exposed loops similar to the CDR1-L and CDR2-L of a $V_L$ (fig. S1). However, as their sequence divergence from antibodies would predict, neither loop adopts any of the known canonical LC CDR structures (*25*). In the pre-BCR structure, the CDR3-L of a $V_L$ is replaced by two unconnected, frayed polypeptide chains comprising the unique regions of λ5 and VpreB (Figs. 1C and 2B and fig. S2). The proteolytic sensitivity of a portion of the λ5 unique region, which is N-terminal to the swapped β strand, suggests that this segment of the molecule is highly accessible and flexible (Fig. 1B). However, we were able to identify 11 ordered amino acids of the C-terminal unique region of VpreB in the electron density maps. This chain protrudes from the antigen-binding site, extends over the top of HC CDR3 (CDR3-H), and obscures the antigen-combining region of the HC (Fig. 2, A and B). The extended VpreB unique region structure is stabilized by a salt bridge between VpreB residue Glu$^{106}$ and HC residue Arg$^{59}$ (asterisk in Fig. 2B), although, as a result of the surface exposure, it may assume alternative conformations when complexed with different HCs [the B factors for this segment are not higher than those of the rest of the structure (table S2)].

We compared the mode of interaction between HC and SLC in the pre-BCR to that between HC and LC of all (seven) antibodies in the Protein Data Bank (PDB) database (Fig. 2C, fig. S2, and table S1) that contain the same number of residues (12) in their CDR3-H as does the HC in our pre-BCR structure. The pre-BCR exhibits a decrease of ~30% in the number of variable domain interface contacts (hydrogen bonds and van der Waals interactions) in comparison to this panel of Fabs (e.g., 53 versus 80 contacts for 1Q0X) and yet buries more surface area than most $V_H/V_L$ pairs (915 Å$^2$ versus an average of 825 Å$^2$) (table S1). This result is due to a net loss of interactions between the SLC and HC framework residues, but there is a gain in the extent of the overall SLC/HC interface due to the SLC unique regions blanketing the HC CDR3-H (Fig. 1B). Consistent with the SLC unique regions probing CDR3-H sequences, we found more contacts (11) between the SLC unique region res-

[1]Program in Immunology, Stanford University School of Medicine, Stanford, CA 94305, USA. [2]Howard Hughes Medical Institute, Stanford University School of Medicine, Stanford, CA 94305, USA. [3]Department of Molecular and Cellular Physiology, Stanford University School of Medicine, Stanford, CA 94305, USA. [4]Department of Structural Biology, Stanford University School of Medicine, Stanford, CA 94305, USA. [5]Department of Microbiology and Immunology, Stanford University School of Medicine, Stanford, CA 94305, USA. [6]Department of Cell Biology, Harvard Medical School, Boston, MA 02115, USA.

*To whom correspondence should be addressed. E-mail: kcgarcia@stanford.edu

idues and CDR3-H than between CDR3-H and CDR3-L in representative Fab structures (an average of four) (table S1).

The CDR3-H loop is extended in the pre-BCR, allowing it to simultaneously interact with SLC CDR2, the unique regions of VpreB and λ5, and other HC framework residues (Fig. 2, B to D). In contrast, in a Fab, the CDR3-H generally makes contact with only a small portion of the $V_L$ CDR1 and CDR2 loops (fig. S3, A and B). The expansive CDR3-H interactions in the pre-BCR are enabled, by fewer structural constraints imposed on the extended and apparently flexible unique regions of VpreB and λ5 (Fig. 2, B and C, and fig. S2B), as compared to the more constrained closed-loop structure of a Fab CDR3-L. Such structural plasticity could permit unique regions to adapt to diverse CDR3-H sequences and loop lengths.

The pre-BCR appears to influence the $V_H$ repertoire (i.e., CDR3-H sequences) of HCs in

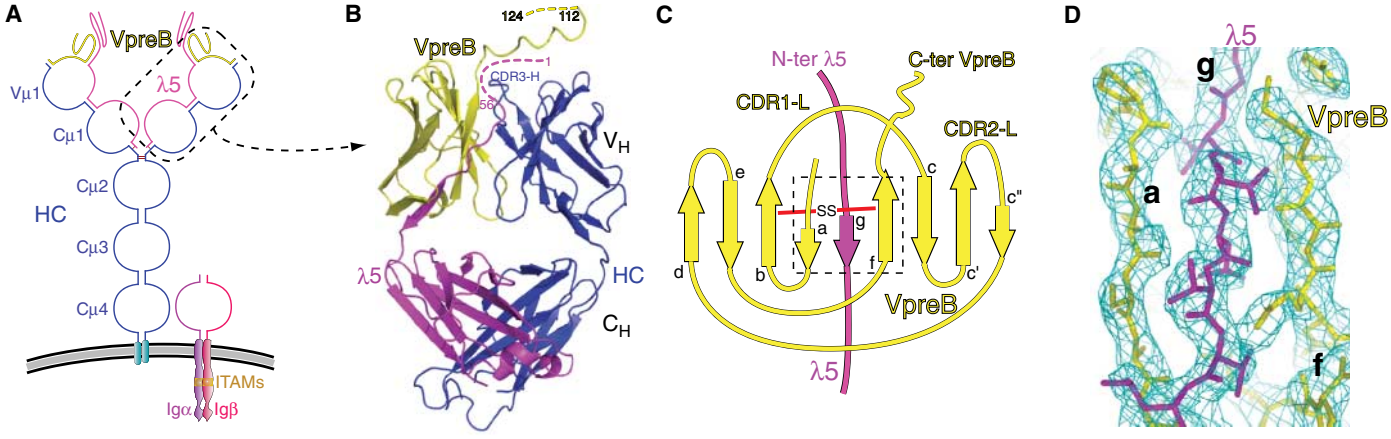


**Fig. 1.** Overall structure of the pre-BCR. (**A**) Cartoon representation of the pre-BCR complex with the Fab-like arm of the pre-BCR that was crystallized (dashed box). (**B**) Ribbon representation of the pre-BCR structure [dashed box in (A)]. Three protein chains are included in the model: VpreB (yellow), λ5 (magenta), and HC (blue). Missing portions of the molecule are indicated with residue numbers and dashed lines at the N terminus of λ5 and the C terminus of VpreB. (**C**) Schematic representation of the V-type Ig fold formed by VpreB and λ5. β strands are designated by arrows labeled a to g. VpreB loops that are homologous to Fab CDRs are labeled. The dashed rectangle indicates the portion of the structure shown in (D). The red line with "SS" indicates the intracellular domain disulfide bond. (**D**) 2.7 Å electron density map ($\sigma_A$-weighted $2F_o - F_c$, where $F_o$ and $F_c$ are the observed and calculated structure factors; contoured to 1.2σ) showing the a and f strands of VpreB and the g strand of λ5.

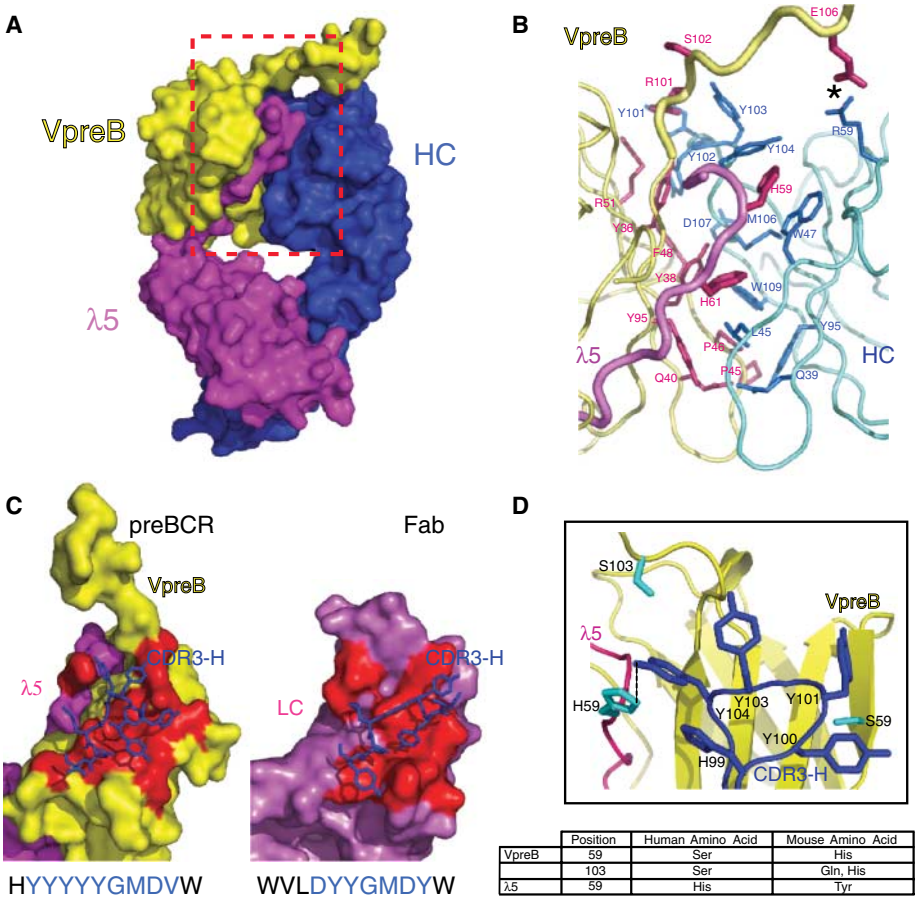


| | Position | Human Amino Acid | Mouse Amino Acid |
|---|---|---|---|
| VpreB | 59 | Ser | His |
| | 103 | Ser | Gln, His |
| λ5 | 59 | His | Tyr |

**Fig. 2.** The pre-BCR CDR3-H sensing site. (**A**) Surface representation of the pre-BCR structure in the same orientation as shown in Fig. 1B. The VpreB unique region exits out the top of the domain, lying over the HC antigen-combining site. (**B**) Contact residues (*29*) within the SLC/HC interface zoomed into the region demarcated by the red dashed box in (A). The main chain is depicted as ribbons with contact residue side chains as sticks. SLC, red; HC, blue. Asterisk designates the interchain salt bridge between VpreB and HC. (**C**) At left, the CDR3-H (blue sticks) from the HC on the surface of the VpreB/λ5 segment of the SLC, showing the extent of interactions between CDR3-H and the VpreB/λ5. The contact footprint between CDR3-H and SLC is highlighted in red. To the right, a similar projection of the CDR3-H on the surface of the LC of a Fab. The contact footprint between CDR3-H and LC is highlighted in red. The CDR3-H sequence is added below both structures with the region shown in sticks highlighted (blue letters). (**D**) Residues demarcating the human pre-BCR CDR3-H sensing site. CDR3-H with side chains (blue), λ5 (magenta), and VpreB (yellow) are shown. Pre-BCR side chains that vary between human and mice and contact CDR3-H are shown in cyan. The dashed line indicates a hydrogen bond. Below the structure, a table of amino acid differences between mice and humans in the region of the CDR3-H sensing site is appended.

the mature B cell population (*11*). We crystallized a human pre-BCR, but the majority of genetic data on HC repertoire selection is derived from murine studies. Comparison of the HC repertoires selected by mouse and human cells reveals that murine CDR3-H sequences contain a significantly higher frequency of tyrosines and are, on average, two amino acids shorter than the human CDR3-H (*26*). The mouse and human VpreB proteins are 73% identical, and the λ5 β-strand insertion is 75% identical. Also, mice have two VpreB proteins (VpreB1 and VpreB2) that are 97% identical, differing at positions 9, 75, and 103 for VpreB1 (Leu$^{9}$, Thr$^{75}$, Gln$^{103}$) and VpreB2 (Ser$^{9}$, Asn$^{75}$, His$^{103}$) from human VpreB (Leu$^{9}$, Thr$^{75}$, Ser$^{103}$). In our pre-BCR structure, positions 9 and 75 are distal to the interface with HC and are therefore unlikely to mediate pre-BCR assembly. The remaining residue, Ser$^{103}$, is located directly above the CDR3-H residue (Tyr$^{104}$) (Fig. 2D) and is therefore close enough to play a structural role in engaging and influencing CDR3-H sequence composition.

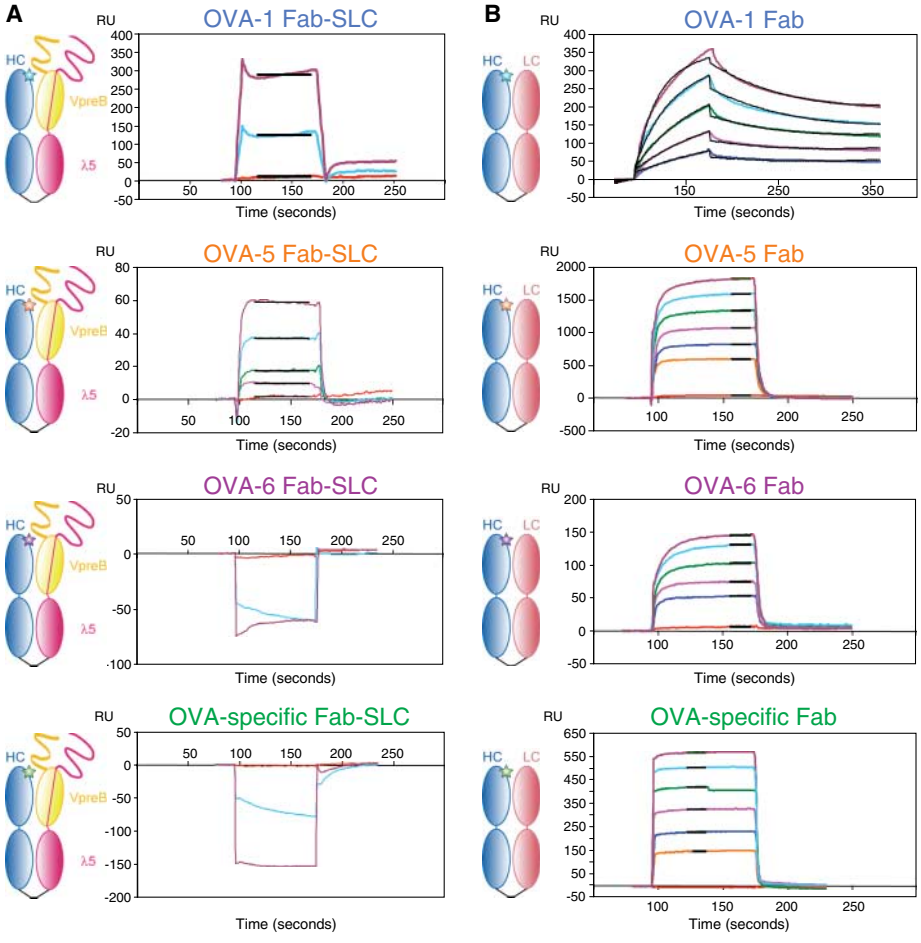


C

| Heavy Chain | CDR3-H Sequence | Fab $K_d$ (μM) | preBCR $K_d$ (μM) |
|---|---|---|---|
| OVA-1* | FRLGMT ------ FDIWGQG | 40 | >>400 |
| OVA-5* | WRYRDWFL ---- FDYWGQG | 9 | 400 |
| OVA-6* | QRITMVRGGMG -FDYWGQG | 11 | NB |
| OVA-specific | HYYYYYG ----- MDVWGQG | 10 | NB |
| HEL-1* | HVRSSSWYFYYGMDVWGQG | NB | NB |

**Fig. 3.** Antigen-binding properties of pre-BCR versus germline Fab. (**A**) SPR sensorgrams for OVA-specific HCs in complex with SLC to form potentially "antigen-specific" pre-BCRs, which we term Fab-SLCs. Four different OVA-specific HCs are paired with SLC. The analyte concentrations shown are 400 (purple), 200 (blue), 100 (green), 50 (magenta), and 0 μM (red). Average resonance unit (RU) fits (horizontal black lines) used for steady-state affinity calculations are shown for the top two panels. CDR3-H differences are denoted by the color of the star in the schematic and the label above the sensorgram. (**B**) SPR sensorgrams for the same four OVA-specific HCs as in (A) but now in complex with the invariant λ1 LC to form a germline Fab that binds to OVA. In the top panel, 1:1 Langmuir binding affinity curve fits are shown, whereas steady-state kinetic fits (horizontal black lines) are shown for all other panels. The analyte concentrations shown are 100 (purple), 50 (light blue), 25 (green), 12.5 (magenta), 6.25 (blue), and 0 μM (red). (**C**) Summary of SPR results. Of the four Fab-SLCs tested, two did not bind, and two others exhibited binding whose affinity was >40 times less than that for the homologous Fab. $K_d$, dissociation constant; NB, no detectable binding. Asterisk indicates HC sequence notation [from (*27*)].

Two pre-BCR residues make extensive contact with CDR3-H in our structure: Ser$^{59}$ in VpreB and His$^{59}$ in λ5 (Fig. 2D). VpreB Ser$^{59}$ interacts with the first two residues of CDR3-H (Tyr$^{100}$ and Tyr$^{101}$), whereas λ5 His$^{59}$ is positioned at the C terminus of CDR3-H, and so together they bracket the CDR3-H. Along with the Ser$^{103}$ position, these residues may demarcate the boundary of a "CDR3-H sensing site" for HC repertoire selection (Fig. 2, C and D). Thus, in tandem with the many complex biological mechanisms that regulate B cell development, we suggest that the SLC unique region residues in proximity to CDR3-H may play a role in influencing the observed sequence differences between the CDR3-H repertoires in mice and humans. The CDR3-H of germline HC is the focal point for sequence diversity, with the rest of the HC and SLC being nonpolymorphic, including interfacial residues between the SLC and the HC. Thus, the site of HC discrimination is likely localized to the CDR3-H.

To address whether the pre-BCR is capable of recognizing antigen, we engineered a pre-BCR by pairing the SLC with an HC of defined antigen specificity. We used OVA-specific germline HCs from genetically limited mice (*IgH*$^{-/-}$ and *Igκ*$^{-/-}$) containing one transgenic human HC locus and the mouse λ LC locus (*27*). The antibodies produced by these mice in response to primary immunization achieve antigen specificity exclusively through different CDR3-H sequences, showing that antigen recognition can be accomplished by diversity in only one of the six CDR loops. For pre-BCR binding experiments, we chose a panel of four OVA-specific HCs from these mice and paired them with an invariant λ1 LC or SLC to produce Fab and pre-BCR, respectively (Fig. 3, A and B). These nonsomatically mutated Fabs recognize OVA with an affinity ranging from 9 to 40 μM by means of surface plasmon resonance (SPR), whereas a hen egg-white lysozyme (HEL)–specific Fab exhibited no detectable binding (Fig. 3, B and C). For pre-BCR complexes of the same HCs and SLC, the highest affinity observed was 400 μM, essentially at the limit of detection for SPR (Fig. 3, A and C). To test the effect of LC diversity, we paired the OVA5 HC with an LC containing a point mutation in CDR3-L and found that the Fab retained binding, confirming the primacy of the CDR3-H in

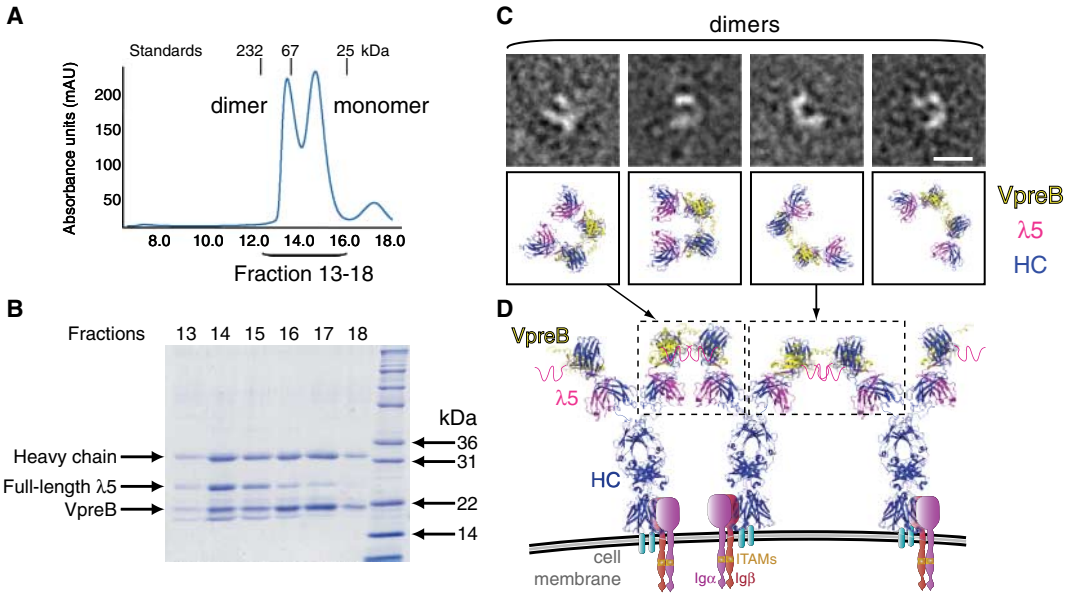


**Fig. 4.** The minimal signaling unit of the pre-BCR is a ligand-independent dimer. (**A**) Pre-BCR with intact SLC unique regions is a dimer. Results of size exclusion chromatography (Superdex-200, Amersham) [with retention volume (ml) on the *x* axis and size standards included] is shown. (**B**) SDS–polyacrylamide gel electrophoresis analysis of the gel filtration demonstrated that the dimeric peak is enriched for full-length λ5, whereas the monomeric peak is deficient in full-length λ5. Truncated λ5 comigrates with VpreB on this gel. (**C**) EM negative stain analysis of dimeric pre-BCR based on ~5400 particles. The top panels show class averages (see Methods and figs. S7 and S8), and the bottom panels show schematic interpretations based on the crystal structure. Scale bar, 10 nm. (**D**) Model of the full-length cell-surface pre-BCR as a signaling active dimer that is consistent with EM and functional studies. The pre-BCR Fab-like dimers resolved by EM are boxed, and the elbow and dimer interface angles are modeled to represent the range of angles observed in EM classes.

antigen recognition (fig. S4) (*28*). These results suggest that the pre-BCR cannot recognize protein antigens in a physiologically meaningful way, but we cannot rule out this possibility for highly abundant antigens or for small molecules. The decrease in antigen binding of the pre-BCR is consistent with the structure of the VpreB C-terminal unique region, which extends over the antigen-combining site and could partially block antigen binding (fig. S5).

Because antigen engagement does not appear to play a role in pre-BCR signaling, we revisited the concept of pre-BCR oligomerization with our recombinant pre-BCR Fab-like fragment. Size exclusion chromatography of the soluble pre-BCR yielded two peaks (Fig. 4A) with HC, λ5, and VpreB in a 1:1:1 stoichiometric ratio, which elute at the positions for a dimer and a monomer, respectively. In the monomer peak, the λ5 unique region was proteolytically truncated (Fig. 4A). Subsequent recombinant truncation of λ5 and VpreB unique regions resulted solely in monomer formation (fig. S6, A and B). Thus, perturbation of the unique regions disrupts dimerization. These data likely explain why a previously reported recombinant form of a pre-BCR Fab-like fragment, in which the VpreB and λ5 were synthetically fused to create a "single-chain" SLC, was a monomer by gel filtration. The ability of the purified recombinant pre-BCR to dimerize indicates that accessory protein(s) are not required for dimerization, and, by extension, pre-BCR signaling through multimerization can occur in a ligand-independent fashion.

Although we were unable to crystallize the dimeric form of the pre-BCR, we undertook electron microscopic (EM) studies of the pre-BCR dimer in negative stain to visualize the oligomeric architecture (Fig. 4C and figs. S7 and S8). A conservative and unbiased analysis of both raw grids and several class averages reveals the pre-BCR dimers (Fig. 4C and figs. S7 and S8), consisting of two pre-BCR monomers (Fab-like modules) connected by a flexible hinge between the tips of the variable domains. The pre-BCR "Fab arms" in each dimer appear constrained to lying on their side, so that we observe a side-on perspective of the interdimer angle (Fig. 4C). The angle between the two pre-BCR molecules ranged from 5° to 60°, suggesting a high level of flexibility at the interface between the two domains. For each pre-BCR dimer class average, we generated a schematic model using the pre-BCR monomer crystal structure (bottom panels in Fig. 4C). We then used the λ5 truncation data, EM results, and the crystal structure to model the pre-BCR signaling complex on the cell surface (Fig. 4D). In this model, each Fab-like arm of the intact pre-BCR on the cell surface dimerizes with that of a different pre-BCR, resulting in an extended chain of self-associated pre-BCRs on the cell surface that could signal through the close proximity of their intracellular domains (Fig. 4D).

### References and Notes


1. C. C. Goodnow, J. Sprent, B. Fazekas de St Groth, C. G. Vinuesa, *Nature* **435**, 590 (2005).
2. S. Tonegawa, *Nature* **302**, 575 (1983).
3. N. Sakaguchi, F. Melchers, *Nature* **324**, 579 (1986).
4. A. Kudo, F. Melchers, *EMBO J.* **6**, 2267 (1987).
5. H. Lanig, H. Bradl, H. M. Jack, *Mol. Immunol.* **40**, 1263 (2004).
6. F. Melchers *et al.*, *Immunol. Today* **14**, 60 (1993).
7. Y. Minegishi, L. M. Hendershot, M. E. Conley, *Proc. Natl. Acad. Sci. U.S.A.* **96**, 3041 (1999).
8. T. Tsubata, M. Reth, *J. Exp. Med.* **172**, 973 (1990).
9. L. M. Hendershot, *J. Cell Biol.* **111**, 829 (1990).
10. S. Pillai, D. Baltimore, *Nature* **329**, 172 (1987).
11. E. ten Boekel, F. Melchers, A. G. Rolink, *Immunity* **7**, 357 (1997).
12. D. J. Decker, N. E. Boyle, J. A. Koziol, N. R. Klinman *J. Immunol.* **146**, 350 (1991).
13. J. Hess *et al.*, *Proc. Natl. Acad. Sci. U.S.A.* **98**, 1745 (2001).
14. H. Karasuyama *et al.*, *Cell* **77**, 133 (1994).
15. U. Keyna, G. B. Beck-Engeser, J. Jongstra, S. E. Applequist, H. M. Jack, *J. Immunol.* **155**, 5536 (1995).
16. M. Milili, C. Schiff, M. Fougereau, C. Tonnelle *Eur. J. Immunol.* **26**, 63 (1996).
17. Y. Minegishi *et al.*, *J. Exp. Med.* **187**, 71 (1998).
18. D. Kitamura *et al.*, *Cell* **69**, 823 (1992).
19. H. Bradl, J. Wittmann, D. Milius, C. Vettermann, H. M. Jack, *J. Immunol.* **171**, 2338 (2003).
20. L. Gauthier, B. Rossi, F. Roux, E. Termine, C. Schiff *Proc. Natl. Acad. Sci. U.S.A.* **99**, 13014 (2002).
21. K. Ohnishi, F. Melchers, *Nat. Immunol.* **4**, 849 (2003).
22. L. D. Wang, M. R. Clark, *Immunology* **110**, 411 (2003).
23. P. Bork, L. Holm, C. Sander, *J. Mol. Biol.* **242**, 309 (1994).
24. A. Kudo, S. Bauer, F. Melchers, *Prog. Immunol.* **7**, 339 (1989).
25. B. Al-Lazikani, A. M. Lesk, C. Chothia, *J. Mol. Biol.* **273**, 927 (1997).
26. M. Zemlin *et al.*, *J. Mol. Biol.* **334**, 733 (2003).
27. J. L. Xu, M. M. Davis, *Immunity* **13**, 37 (2000).
28. M. M. Davis, *Semin. Immunol.* **16**, 239 (2004).
29. Single-letter abbreviations for the amino acid residues are as follows: A, Ala; C, Cys; D, Asp; E, Glu; F, Phe; G, Gly; H, His; I, Ile; K, Lys; L, Leu; M, Met; N, Asn; P, Pro; Q, Gln; R, Arg; S, Ser; T, Thr; V, Val; W, Trp; and Y, Tyr.


30. We thank M. Conley for providing human SLC cDNA; M. Krogsgaard for assistance with SPR; M. Boulanger, P. Strop, and X. Wang for assistance with x-ray crystallography; and M. Winslow and L. Colf for critical reading of the manuscript. This work was supported by grants from NIH, Keck Foundation, and Howard Hughes Medical Institute (K.C.G.) and the Stanford Immunology Program Training Grant (A.J.B.). The molecular EM facility at Harvard Medical School was established with a generous donation from the Giovanni Armenise Harvard Center for Structural Biology and is maintained with funds from NIH (to T.W.). Coordinates and structure factors have been deposited in the PDB (www.rcsb.org) with accession number 2H32.


### Supporting Online Material

www.sciencemag.org/cgi/content/full/316/5822/291/DC1
Materials and Methods
SOM Text
Figs. S1 to S8
Tables S1 to S3
References

29 December 2006; accepted 13 March 2007
10.1126/science.1139412